tegration over $d^m\mathbf{R}$ gives the final result, eq 12.

References and Notes

(1) Y. Oono, *J. Phys. Soc. Jpn.*, **41**, 2095 (1976).
(2) T. Oyama and Y. Oono, *J. Phys. Soc. Jpn.*, **42**, 1348 (1976).
(3) H. Yamakawa, "Modern Theory of Polymer Solutions", Harper and Row, New York, 1971.
(4) J. G. Kirkwood, *Recl. Trav. Chim. Pays-Bas* **68**, 649 (1949).
(5) J. G. Kirkwood, *J. Polym. Sci.*, **12**, 1 (1954).
(6) M. Fixman, *J. Chem. Phys.*, **23**, 1656 (1955).

Polymer Self-Diffusion: Dynamic Light Scattering Studies of Isorefractive Ternary Solutions†

James E. Martin

Division 1152, Sandia National Laboratories, Albuquerque, New Mexico 87185.
Received July 9, 1983

ABSTRACT: Dynamic light scattering measurements are reported for the ternary system poly(vinyl methyl ether) (PVME)/polystyrene (PS)/toluene. PVME is index matched by toluene, and hence scatters very little light, over a wide concentration range. Thus it is shown that dynamic light scattering can be used to measure the self-diffusion coefficient of PS ("optically labeled") chains. Since PS is chemically different from PVME, a scaling treatment is given for the concentration and molecular weight dependence of D in ternary systems. Simple power law behavior is not found for the concentration dependence but the molecular weight dependence is predicted to be $D \sim M^{-9/5}$. The scaling analysis also shows a crossover, beyond the semidilute crossover, from Stokes–Einstein diffusion to reptation. This dynamical crossover depends on the relative molecular weights of the labeled and "solvent" chains and is derived for chemically identical and nonidentical chains in both good and Θ solvents. The experimental data substantiate the scaling results; the crossover to reptation for the ternary system studied is at ca. 15% volume fraction PVME whereas the semidilute crossover for PVME was found from viscosity data to be at a volume fraction of 4%.

Introduction

The reptation model[1] provides a simple and appealing description of the diffusion of polymers in highly congested solutions. To date there have been a number of experiments which indicate that reptation ideas are essentially correct. The methods brought to bear on this problem are extensive: forced Rayleigh scattering,[2] pulsed field gradient nuclear magnetic resonance,[3,4] luminescence quenching,[5] slow-mode analysis of dynamic light scattering data,[6,7] radioactive tracers,[8,9] and infrared spectroscopy from deuterium-labeled chains.[10] The purpose of this paper is to introduce a new method for the study of the dynamics of highly entangled labeled chains: dynamic light scattering from isorefractive ternary solutions. The idea of optically labeled chains is simple enough and is certainly not new,[11] but the application of dynamic scattering techniques to such systems has not been reported in the literature.

Isorefractive scattering is the optical analogue of neutron scattering from deuterium-labeled chains; the ternary system consists of a solvent (toluene), a large concentration of index-matched polymer (poly(vinyl methyl ether) (PVME)), and a very small concentration of "labeled" polymer (polystyrene (PS)) with a large refractive index increment. There are, of course, some considerations in devising such a system. First, the ternary system must be compatible over a wide range of index-matched polymer concentration. Second, the index-matched polymer must be index matched over this concentration range. The system PS/PVME/toluene fulfills these requirements quite well, being much more compatible than the system PS/PMMA/toluene, for which static light scattering data have been reported[12].

Dynamic light scattering is ideally suited to the study of single-chain dynamics and offers some advantages over other techniques. First, a very broad spatial (ca. 25–500 nm) and temporal range (ca. 1 μs to 1 s) can be probed. Thus not only can reptation be investigated, but internal modes of entangled single chains can be studied—an experiment that previously has only been possible with spin-echo neutron scattering.[13] Second, the measurements are quickly and easily made, and samples are easily prepared, requiring only filtering and mixing. It should be pointed out, however, that there is an important disadvantage in working with ternary systems; power law scaling behavior does not hold for some of the properties of these chemically nonidentical chains (see below).

In this paper preliminary results are given for the concentration and wavevector dependence of the apparent diffusion coefficient in a system in which the labeled chains (M_n = 900 000) are longer than the isorefractive chains (M_v ~ 110 000). The applicability of scaling results to this system is discussed, with particular consideration given to thermodynamic screening and the crossover from Stokes–Einstein diffusion to reptation. Power law behavior is not expected for the concentration dependence of D but is predicted for the molecular weight dependence, with minor alteration of the exponent. Too, the crossover to reptation is predicted to occur well beyond the semidilute crossover for the semidilute chains. This prediction is verified by the experimental data.

Experimental Section

Equipment. Self-diffusion coefficients were determined on a photon correlation spectrometer that has not yet been described in the literature. The apparatus consists of the following components: a Spectra-Physics Model 125A He–Ne laser, a Spectra-Physics Model 164 argon ion laser, an Aerotech goniometer (which can be step scanned to a resolution of 0.9 MOA), a Malvern photomultiplier tube housing, an amplifier–discriminator unit, an index-matched sample cell assembly, an ITT FW130 photomultiplier tube (selected for low after-pulsing), a 72 hardware channel Model 1096 Langley-Ford correlator, and a DEC LSI 11/23 computer. The purpose of the computer is twofold: analysis of the data (single- and double-exponential decay nonlinear fitting routines, with or without a floating base line, and a cumulants

†This work performed at Sandia National Laboratories supported by the U.S. Department of Energy under Contract No. DE-AC04-76DP00789.

0024-9297/84/2217-1279$01.50/0

Table I
Samples

sample	vol fraction of polymer, %	wt fraction of polystyrene, %
1	2.43	0.2
2	4.91	0.2
3	7.34	0.2
4	9.53	0.2
5	11.24	0.2
6	14.03	0.2
7	16.66	0.2
8	19.00	0.2
9	21.19	0.2
10	22.46	0.2
11	26.15	0.2
12	2.23	0
13	5.03	0
14	6.94	0
15	9.33	0
16	11.64	0
17	14.39	0
18	16.25	0
19	18.67	0
20	20.80	0
21	23.31	0

program) and complete automation of the spectrometer. The lasers are aligned so that after passing through a beam splitter cube the beams are coaxial. This feature allows investigation of a large region of wavevector space with a single detection system.

Viscosity measurements were made with a range of Cannon-Ubbelohde viscometers.

Materials. The polystyrene was obtained from Pressure Chemical Co. (lot no. 80323) of nominal M_n = 900 000 and polydispersity index 1.10. The poly(vinyl methyl ether) (PVME) was obtained from GAF (Gantrez M-556). Gel permeation chromatography indicated that the PVME was fairly polydisperse. Intrinsic viscosity data gave a molecular weight of 110 000.

Preparation. PVME was diluted with toluene to ca. 15 wt % polymer and prefiltered through a 3-μm Millipore MF filter. This solution was then injected through a 0.45-μm MF filter into ca. 25-mL sample containers. GPC analysis on the filtered PVME indicated no decrease in the polymer molecular weight due to scission in the filtering process. After these samples were weighed, a polystyrene solution (20.0 mg/mL) was injected into each sample through a 0.45-μm MF filter. The quantity of PS solution was chosen to give a final PS concentration of 0.2 mg/mL. The semidilute crossover for polystyrene of this molecular weight is ~17 mg/mL. The final concentrations, shown in Table I, were attained by either diluting the samples with 0.2-μm-filtered toluene or slowly evaporating the samples in a dust-free oven with a steady circulation of 0.2-μm-filtered air. Final concentrations were determined gravimetrically and samples showing signs of dust were discarded. Volume fractions were calculated from the gravimetric data using 1.154 and 0.98 mL/g for the specific volumes of toluene and PVME, respectively. These data are shown in Table I.

Scattering Measurements. Vertically polarized scattered light from the He–Ne laser was detected at a number of angles and, after discrimination, was sent to the correlator for processing. The delay time per correlator channel was fixed so that the correlated part of the signal had decayed to $1/e$ after ~14 channels. In practice, this was accomplished by adjusting the sample time at 90° to satisfy this criterion and then letting the automation software compute the sample time at other angles, based on inverse q-squared dependence of the relaxation time. The homodyne correlation functions were then sent to the computer, archived on floppy disks, and analyzed by a variety of fitting routines.

Results

Typical correlation functions for a dilute and a concentrated sample, respectively, are shown in curves a and c of Figure 1 along with single-exponential fits to these data. The residuals show a systematic deviation from single-exponential behavior, attributable to configurational

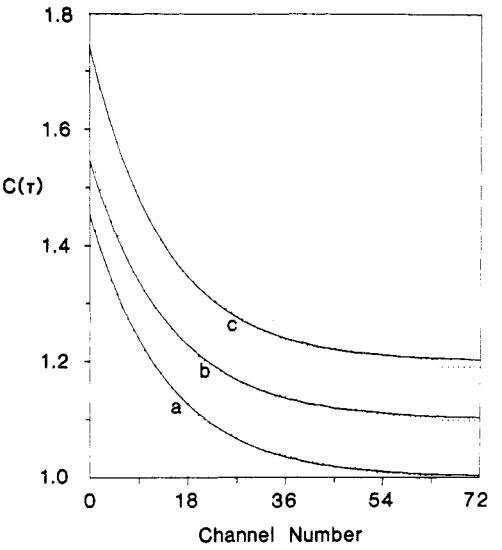

Figure 1. Homodyne intensity autocorrelation functions are plotted with curves b and c displaced by 0.1 and 0.2, respectively. These data were taken at 90° with the He–Ne laser: (a) data for sample no. 1 are force fit to a single exponential, and the delay time per channel is 0.015 ms; (b) these data are fit with the first six channels deleted—this decreased the apparent diffusion coefficient by 4%; (c) the data for sample no. 11 are fit to a single exponential, and the delay time per channel is 2.5 ms.

diffusion of the polymer. In fact, the radius of gyration of the PS used in this study is ca. 45 nm in pure toluene and the magnitude of the reciprocal wavevector varied from ca. 39 to 130 nm. Thus at large angles configurational diffusion contributed a low-amplitude, rapidly decaying component to the intensity autocorrelation function; at small angles this effect vanished.

Two methods were used to extract the self-diffusion coefficient from the data. In the first method a number of initial channels of the correlation function (typically six) were excluded from a nonlinear fit to the homodyne function

$$C(t) = A \exp(-2Dq^2t) + B \quad (1)$$

The base line, B, was allowed to "float" and then compared to the value given by the correlator. In this expression q is the scattering wavevector and has a magnitude $4\pi \sin(\theta/2)/\lambda'$, where θ is the scattering angle and λ' is the optical wavelength in the scattering medium. This fitting procedure serves as a check on dust contamination in the samples—large amounts of dust will give a value of B that is substantially larger than the machine-given base line. In general, the machine base line and the parameter B agreed to within 0.2%. Figure 1b shows the correlation function of Figure 1a fit in this way.

Homodyne scattering has not always been assumed for concentrated polymer solutions.[6,7] In such solutions small heterogeneities can act as a source of stray light and induce some degree of heterodyning. In these samples the assumption of homodyning is supported by two observations: (1) the intensity of scattered light did not vary throughout the entire range of PVME concentrations, from dilute to concentrated; (2) heterodyning could be induced by moving the detector to small angles where there is stray light due to imperfections in the sample cells.

In the second method of data analysis the correlation functions were fit to the double-exponential homodyne function

$$C(t) = (A \exp(-t/\tau_1) + E \exp(-t/\tau_2))^2 + B \quad (2)$$

Here, $\tau_1 = 1/Dq^2$ and $\tau_2^{-1} = \tau^{-1} + Dq^2$, where τ is the

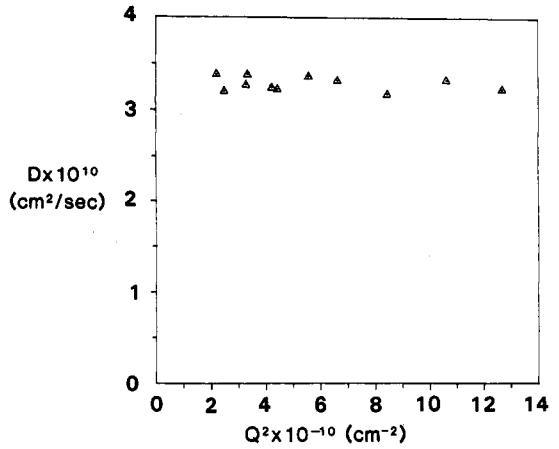

Figure 2. q dependence of the apparent diffusion coefficient of sample no. 11.

relaxation time associated with configurational diffusion. These parameters were evaluated with a nonlinear least-squares program that fits eq 2 directly to the homodyne data, with either four or five parameters depending on whether the base line is allowed to float. In fact, two decay times could be extracted from the data at all concentrations; these decay times and their amplitudes were essentially unchanged by floating the base line. The ratio of the slow time to the fast time was ca. 3.5–4 throughout the concentration range and the relative amplitude of the fast component decreased with concentration to ca. 1% (homodyne amplitude) in the most concentrated solution. The two methods of data reduction agreed in all cases to within 3% on the same data set.

The q dependence of the apparent diffusion coefficient is shown in Figure 2 for sample no. 11. These data were taken with both the He–Ne (λ = 632.8 nm) and argon ion lasers (λ = 514.5, 488.0, and 457.9 nm) and span a fairly large region of wavevector space. No real q dependence was observed for this sample, at least in the range of the available data. At smaller wavevectors the presence of some dust in the samples prevented obtaining reliable data. The scatter in the data indicates a relative error of ca. 5% in D. Index matching of the PVME was sufficiently good that autocorrelation functions could not be obtained for the control samples (samples 12–21).

Figure 3 shows the dependence of D on the volume fraction of polymer. The line tangential to the data is the scaling prediction for the self-diffusion coefficient for a good solvent binary system[1]

$$D_r \sim M^{-2}\phi^{-7/4} \tag{3}$$

and is included primarily for comparison. Clearly, the data in Figure 3 do not show power law behavior but decrease faster than any power law. This can be understood in terms of a crossover from Stokes–Einstein diffusion to reptation.

Scaling in Bimodal Solutions

There are two reasons why eq 3 is inapplicable to the ternary system studied here. First, the labeled chains are much longer than the isorefractive chains. Second, the isorefractive chains are not chemically identical with the labeled chains; thermodynamic screening does not apply to the PS molecules. Daoud and de Gennes have treated the dynamics of bimodal melts[14] and have concluded that although tube renewal is an insignificantly slow process, Stokes–Einstein diffusion is not. It is not difficult to extend the treatment of Daoud et al. to ternary solutions consisting of a bimodal distribution of chemically identical

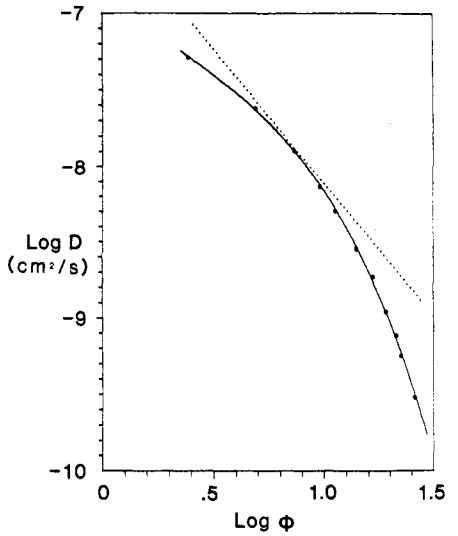

Figure 3. Diffusion coefficient shown as a function of the percent volume fraction. The solid line is a quartic fit to the data and the dotted line has a slope of −1.75.

or nonidentical chains in good or Θ solvents.

A. Stokes–Einstein/Reptation Crossover ϕ_r. Consider a solution that is very dilute in long chains of N monomers and semidilute in short chains of P monomers. By very dilute we mean that the long chains make a negligible contribution to the solution viscosity. In the usual way the reptation self-diffusion coefficient, D_r, of the long chains can be expressed in terms of the reptation time, $\tau_r(N)$, and the radius, R.[1]

$$D_r \sim R^2/\tau_r(N) \tag{4}$$

The expression for the Stokes–Einstein diffusion coefficient of these long chains is just

$$D_s \simeq T/6\pi\eta_p R \tag{5}$$

where η_p is the solution viscosity and T has units of energy. The scaling expression for the viscosity[1] is

$$\eta_p \sim E\tau_r(P) \sim (T/\xi^3)\tau_r(P) \tag{6}$$

where E is the osmotic modulus, $\tau_r(P)$ is the reptation time for the short chains, ξ is the radius of a concentration blob (determined essentially by the short chains), and g is the number of monomers within a concentration blob. The ratio of the reptation to the Stokes–Einstein diffusion coefficient is

$$\rho \equiv D_r/D_s \sim (RP/N\xi)^3 \tag{7}$$

It is reasonable to define the crossover ϕ_r by the concentration at which $\rho = 1$. At concentrations exceeding this, reptation is faster than Stokes–Einstein diffusion and will dominate.

Equation 7 can be evaluated for a number of specific cases.

These include the following:

(i) Good solvent, chemically identical chains with screened interactions. Here the temperature blob is much smaller than the concentration blob defined by the chains of P monomers. It has been shown by Joanny et al.[15] that there is a swollen/ideal crossover, ϕ^+, for the long chains for $P > N^{1/2}$. This crossover occurs at a concentration that is greater than the semidilute crossover for the short chains. At concentrations exceeding ϕ^+ long-range interactions are screened and the long chains are ideal. Since reptation is probably not an important process when $P < N^{1/2}$ we do not examine this case.

(ii) Good solvent, chemically identical chains below ϕ^+ or chemically nonidentical chains. Here the interactions are not screened either due to ϕ being less than ϕ^+ or due to chemical differences in the P and N chains.

(iii) Θ solvent, chemically identical chains. Here interactions are screened and the long chains are ideal.

Case i. In good solvents the concentration blob ξ is known to scale as $\phi^{-3/4}$.[1] Since interactions on the long chains are screened ($\phi > \phi^+$) the long-chain radius obeys the ideal law $R \sim N^{1/2}$, but the blobs are swollen and $\xi \sim g^{3/5}$. Substitution of these quantities into eq 7 with $\rho = 1$ gives the reptation crossover.

$$\phi_r \sim (N^{1/2}/P)^{8/5} \tag{8}$$

Of particular interest is the unimodal limit, $P = N$. The reptation crossover (a dynamical crossover) for this binary system is then seen to occur at the semidilute (thermodynamic) crossover.

$$\phi_r \sim \phi^* \sim N^{-4/5} \tag{9}$$

Since the reptation crossover for the long chains occurs at higher concentration than the semidilute crossover for the short chains, there is no inconsistency in using eq 6 for bimodal systems. However, in the unimodal case an underlying assumption is that the viscosity crossover occurs at a concentration that is lower than or equal to the reptation crossover. It is not clear that this assumption is valid.

Case ii. The extension to chemically different chains is simple enough; here interactions between blobs on the long chains (PS) are not screened by the presence of the short chains (PVME). Thus the concentration dependence of the radius is complex (see below) and power law behavior is not expected. In general, the long chains will be swollen on both short-length scales ($\xi \sim g^{3/5}$) and long-length scales ($R \sim N^{3/5}$). The Stokes–Einstein/reptation crossover is just

$$\phi_r \sim (N^{2/5}/P)^{4/3} \tag{10}$$

Qualitatively the situation is much the same as for chemically identical chains, the change in exponents being small.

Case iii. Finally, we predict the reptation crossover in Θ solvents. Here the static correlation length, ξ, scales like $1/\phi$, the number of monomers per blob is given by $\xi^2 \sim g$, and $R \sim N^{1/2}$. Combining these gives

$$\phi_r \sim (N^{1/2}/P) \tag{11}$$

Again it is interesting to examine the unimodal limit $P = N$. Again the dynamical crossover occurs at the semidilute crossover

$$\phi_r \sim \phi^* \sim N^{-1/2} \tag{12}$$

From this qualitative analysis an obvious conclusion can be drawn; the study of reptation in bimodal solutions favors large P. Too, N must be sufficiently large that the reptation crossover is far below the end of the semidilute regime (where the concentration blob is smaller than a Kuhn statistical segment) and the radius of the labeled chains must be much larger than the static correlation range of the solvent chains. In good solvents with N small it is additionally possible that the reptation crossover could occur beyond the marginal crossover.

B. Concentration and Molecular Weight Dependence of D. Equation 4 gives D_r in terms of the reptation time and the polymer radius. The reptation time is defined as the time it takes a polymer with tube diffusion coefficient D_t to diffuse out of its original tube of contour length L_t.

$$\tau_r \sim L_t^2/D_t \sim (Ng^{-1}\xi)^2/(\mu_b T/Ng^{-1}) \tag{13}$$

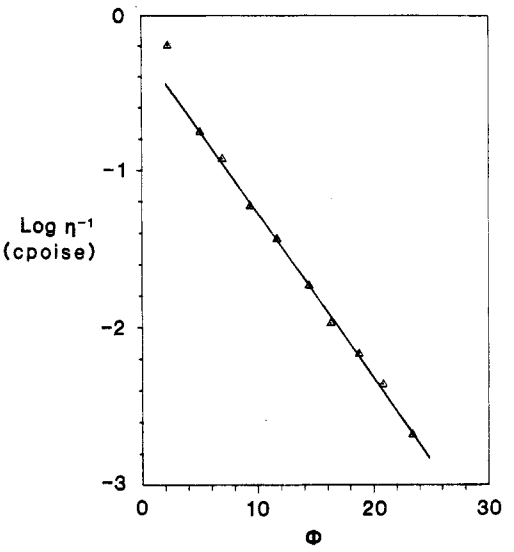

Figure 4. Contribution of PVME to the solution viscosity (the solvent part has been subtracted from these data), taken at 27 °C. The data are exponential beyond the semidilute concentration.

The number of blobs in a tube is N/g, so $L_t = Ng^{-1}\xi$. The tube diffusion coefficient, in terms of the blob mobility μ_b, is $\mu_b T/Ng^{-1}$. Using $\mu_b \sim 1/\eta\xi$ to express the blob mobility in terms of the solvent viscosity and the blob radius gives an expression for D_r. Retaining only the concentration and molecular weight dependence,

$$D_r \sim R^2\xi^2/N^3 \tag{14}$$

For good solvents and chemically identical chains (case i above) the canonical screening argument $R^2 \sim (N/g)\xi^2$ applies. Using $\xi \sim g^{3/5}$, the scaling law for the concentration dependence of the radius is $R^2 \sim N\xi^{1/3} \sim N\phi^{-1/4}$. With eq 14 this gives the well-known result[1]

$$D_r \sim N^{-2}\xi^{7/3} \sim N^{-2}\phi^{-7/4} \tag{15}$$

For chemically nonequivalent chains (case ii above) screening does not apply, and the polymer is swollen on length scales greater than the thermal blob radius. The polymer radius can then be expressed in terms of the binary cluster integral, v, as for dilute polymers in good solvents.[16]

$$R^2 \sim N^{6/5}v^{2/5} \tag{16}$$

The concentration dependence of v will generally be complex and scaling arguments can make no predictions about this. Certainly simple power law behavior is not expected for the radius in the semidilute regime. Equations 14 and 16 give

$$D_r \sim N^{-9/5}\phi^{-3/2}v^{2/5} \tag{17}$$

for the dependence of D_r on ϕ and N. Scaling behavior is still expected for the molecular weight dependence, but the concentration dependence is not amenable to a scaling analysis.

Discussion

Figure 4 shows the dependence of the solution viscosity on the volume fraction of PVME. These data were obtained from samples 12–21. The PVME was polydisperse and power law behavior was not observed for the viscosity. Instead, for volume fractions exceeding ca. 5% the viscosity increased exponentially with concentration. To obtain an estimate of the semidilute crossover for PVME in toluene the relation $c \sim 3/[\eta]$ was used.[17] Measurements on ad-

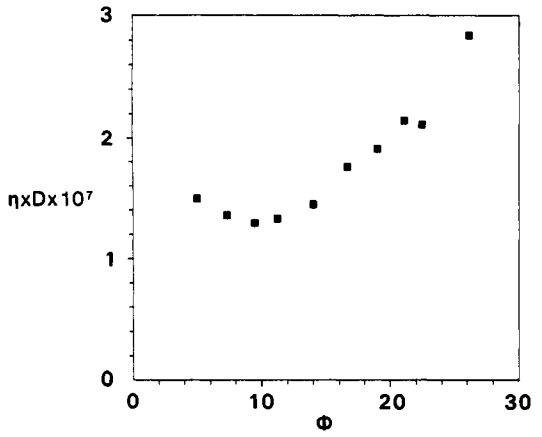

Figure 5. Product of diffusion coefficient and solution viscosity plotted vs. percent volume fraction.

ditional dilute samples (volume fractions less than 2%) gave $[\eta]$ = 0.80 dL/g so the semidilute crossover occurs at a volume fraction of ca. 4%.

The crossover from Stokes–Einstein diffusion to reptation is apparent in Figure 5, where the product $\eta_p D$ is plotted against concentration. Apparently, Stokes–Einstein diffusion dominates until the volume fraction exceeds ~14%. At this concentration the PVME is well into the semidilute regime as predicted above. Looking again at Figure 5, one sees that Stokes–Einstein diffusion dominates well past the concentration where the slope is −1.75. Further, the data in Figure 5 admit to an alternative explanation; it is conceivable that Stokes–Einstein diffusion dominates the entire concentration range, and the upturn in the data of Figure 5 represents a collapse in the hydrodynamic radius.

A comment should be made about the slow mode reported by Amis et al.[6,7] in dynamic light scattering studies of semidilute solutions. Originally this slow mode was attributed to self-diffusion since the expected concentration and molecular weight scaling behavior was observed. Recently, however, Chang and Yu have reported[18] that the diffusion coefficients derived from the slow mode of the autocorrelation function differ by an order of magnitude from the diffusion coefficients derived from forced Rayleigh scattering (FRS) measurements (pigskin gelatin). This has shed some doubt as to the real nature of the slow mode. Should the slow mode be attributed to self-diffusion? The experimental evidence is compelling—perhaps the problem is simply one of scale. The fringe spacing in the FRS study was typically several microns whereas in the DLS measurements the probe length was typically less than 100 nm. When the probe size is comparable to macromolecular dimensions, it is questionable whether or not macroscopic diffusion is being measured in a reptating system. Indeed, it may well be the case that the fractal dimension of the center of mass trajectory is no longer 2 on such a small spatial/time scale. The study of isorefractive systems, where it is certain that center of mass diffusion is measured, should resolve the question of the proper interpretation of the slow mode, once comparison is made to FRS measurements on the same system.

Conclusions

A new technique has been described for measuring self-diffusion of polymers in entangled solutions. The technique offers new possibilities for probing the internal motions of entangled chains—a subject of current theoretical interest. Preliminary results on the concentration dependence of self-diffusion of PS in PVME/toluene solutions indicate that Stokes–Einstein diffusion can be an important process in the semidilute regime. The scaling arguments presented here are only approximate but they do indicate that dynamical crossovers can occur at much larger concentrations than the static semidilute crossover. Future experiments on these ternary systems will include small-angle X-ray scattering measurements on PVME/toluene solutions to determine the static correlation range and measurements of the concentration dependence of the PS static radius to determine whether the upturn of the data in Figure 5 is due to a reptation crossover or a collapse in the hydrodynamic radius.

Experiments have been initiated on polystyrene/butadiene stars and on the PS molecular weight dependence of the apparent reptation crossover. Too, the study of the dynamics of internal motions of high molecular weight polystyrene in concentration PVME/toluene solutions has begun and should illuminate this relatively new area of research.

There are a number of interesting experiments that can be done with optically labeled chains. Hopefully these experiments will lead to increased insight into the dynamics of single chains in entangled solutions.

Registry No. PVME (homopolymer), 9003-09-2; PS (homopolymer), 9003-53-6.

References and Notes

(1) P.-G. de Gennes, "Scaling Concepts in Polymer Physics", Cornell University Press Ltd., London, 1979, p 223.
(2) L. Leger, H. Hervet, and F. Rondelez, *Macromolecules*, **14**, 1732 (1981).
(3) P. T. Callaghan and D. N. Pinder, *Macromolecules*, **14**, 1334 (1981).
(4) W. Brown and P. Stilbs, *Polymer*, **24**, 188 (1983).
(5) I. Mita, K. Horie, and M. Takeda, *Macromolecules*, **14**, 1428 (1981).
(6) E. J. Amis and C. C. Han, *Polymer*, **23**, 1403 (1982).
(7) E. J. Amis, P. A. Janmey, J. D. Ferry, and H. Yu, *Macromolecules*, **16**, 441 (1983).
(8) F. J. Bueche, *J. Chem. Phys.*, **48**, 1410 (1968).
(9) Y. Kumagai, H. Watanabe, K. Miyasaka, and T. Hata, *J. Chem. Eng. Jpn.*, **12**, 1 (1979).
(10) J. Klein and B. J. Briscoe, *Proc. R. Soc. London, Ser. A*, **365**, 53 (1979).
(11) P. Kratochvil, B. Sedlacek, D. Strakova, and Z. Tuzar, *Makromol. Chem.*, **166**, 265 (1973).
(12) C. Y. Lin and S. L. Rosen, *J. Polym. Sci., Polym. Phys. Ed.*, **20**, 1497 (1982).
(13) D. Richter, A. Baumgartner, K. Binder, B. Ewen, and J. B. Hayter, *Phys. Rev. Lett.*, **47**, 109 (1981).
(14) M. Daoud and P.-G. de Gennes, *J. Polym. Sci., Polym. Phys. Ed.*, **17**, 1971 (1979).
(15) J. F. Joanny, P. Grant, P. Pincus, and L. A. Turkevich, *J. Appl. Phys.*, **52**, 5943 (1981); *J. Phys. (Paris)*, **42**, 1045 (1981).
(16) H. Yamakawa, "Modern Theory of Polymer Solutions", Harper and Row, New York, 1971.
(17) H. L. Frisch and R. Simha, "Rheology", Academic Press, New York, 1956.
(18) T. Chang and H. Yu, paper submitted to *Macromolecules*.